

MODELLING OF CLIMBING FILM EVAPORATORS

¹SD PEACOCK AND ²M STARZAK

¹Sugar Milling Research Institute, University of Natal, Private Bag X10, Dalbridge, 4014

²University of Natal, Durban

Abstract

Climbing film evaporators are widely used in the South African sugar industry. However, it is generally considered that the performance of these evaporators could be improved. Unfortunately, very little design information is available in the literature, making it difficult to predict the effects of altered operating conditions on evaporator performance. A mathematical model of the climbing film evaporator system was developed as a simulation tool for evaporator designers and operators. The basis of the mathematical model is briefly outlined, and the results of preliminary investigations into evaporator simulation are reported. The testing of the model against experimental data from the Felixton pilot plant climbing film evaporator is discussed, and improvement of the model by process identification is described. Further potential uses of the model are outlined.

Keywords: Evaporators, climbing film, modelling, simulation, optimisation

Introduction

In recent years there has been concern that the evaporator stations at some South African sugar mills are not performing optimally. A thorough investigation of the problem has been hampered by difficulty in obtaining reliable and reproducible experimental data under specific operating conditions. A project was thus launched to examine the performance characteristics of long-tube climbing film evaporators by both experimental study and modelling. The results of the experimental programme are discussed elsewhere (Walthew *et al.*, 1995; Walthew and Whitelaw, 1996). In this paper, the mathematical modelling of climbing film evaporators is described. The results of the modelling are compared with those obtained by experiment from the Felixton pilot plant climbing film evaporator. The use of the model for process optimisation is discussed.

The mathematical model

Despite the industrial importance of climbing film evaporators, there are relatively few papers in the literature in which their performance was simulated using a rigorous mathematical model of the evaporation process. In the early studies by Gupta and Holland (1966), the evaporator was considered as a lumped-parameter system and mutual relations between process variables averaged over the entire apparatus were discussed. The first distributed-parameter model accounting for the distribution of temperature, pressure and juice composition over the length of the tubes was due to Bourgois and Le Maguer (1983). This model, however, was based on several simplifying assumptions, among which the constant evaporation rate along the tubes seems to be its most serious drawback. In 1984, Zinemanas *et al.* performed a very general study on the simulation of heat exchangers with change of phase, allowing for multicomponent phase equilibria. In principle, the model which will be presented

here follows the modelling concepts formulated therein.

The system to be modelled is that of a climbing film evaporator, as shown in Figure 1. Juice is fed to the preheater, where it is heated to the required feed temperature. The hot juice is then fed to the bottom of the evaporator tubes. For the purposes of modelling, the cane sugar juice fed to the evaporator is assumed to be a three-component mixture, consisting of water, sucrose and non-sucrose dissolved solids. It is further assumed that the following quantities are known under any given set of evaporator operating conditions, and can be assigned numerical values (Figure 1):

- the flow rate of 'cold' juice to the preheater (F_0)
- the sucrose content of the feed stream to the preheater (s_0)
- the non-sucrose solids content of the feed stream to the preheater (r_0)
- the temperature of the hot juice leaving the preheater, before entering the bottom of the evaporator tubes (T_{L0})
- the vapour space pressure at the top of the evaporator tubes (P_{top})
- the flowrate of condensate (per unit width) at the top of the tubes (Γ_0). This is taken to be zero, as there is assumed to be no condensate film at the very top of the tube.

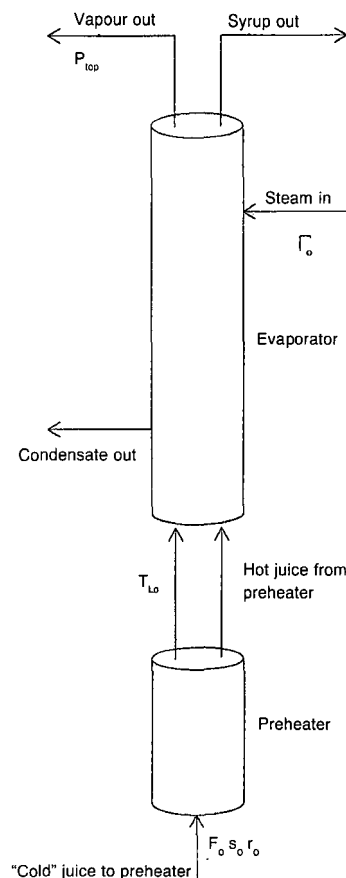


FIGURE 1: The climbing film evaporator system.

Modelling of the steady state adiabatic operation of the evaporator results in a set of six ordinary differential equations; namely, total (juice and vapour mixture) enthalpy and mass balances within the tube (equations 1 and 2, respectively), two individual component mass balances (sucrose and non-sucrose dissolved solids – equations 3 and 4 respectively), a condensate enthalpy balance (equation 5) and a momentum balance for the juice and vapour within the tube (equation 6):

$$\frac{dH}{dz} = \pi D_{in} q_{conv}, \text{ where } q_{conv} = \alpha_L (T_{w2} - T_L) \quad (1)$$

$$\frac{d(L + V)}{dz} = \frac{d(Ls)}{dz} = \frac{d(Lr)}{dz} = 0 \quad (2), (3), (4)$$

$$\frac{dH_c}{dz} = -\pi D_{out} q_{condens}, \text{ where } q_{condens} = \alpha_c (T_s - T_w) \quad (5)$$

$$\frac{d\bar{p}}{dz} = \left(\frac{dp}{dz} \right)_{friction} - \rho_m g, \text{ where } \bar{p} = p + \frac{F_b^2}{A^2 \rho_m} \quad (6)$$

The heat flux across a tube at a given vertical position in the evaporator depends on the temperature distribution across the pipe wall and the two adjacent fluid films (condensate and juice). This temperature distribution can be determined from the following heat flux conservation conditions:

$$q_{condens} D_{out} = q_{conduct} D_{out} = q_{conv} D_{in} \quad (7)$$

The differential equations (2), (3) and (4) are trivial and can be solved analytically. A combination of equations (1), (5) and (7) is also integrable, resulting in a simple explicit relationship between the enthalpy flow rate of condensate, H_c , and that of the juice and vapour mixture, H . The remaining equations, involving the two state variables: enthalpy (H) and pressure (p), (1) and (6), can only be approached numerically, taking advantage of the available analytical solutions of the other differential equations.

The rate data required for the evaluation of the right hand sides of the remaining two ordinary differential equations and for the algebraic solution of equation (7) were determined as follows:

- *viscous pressure drop* $[(dp/dz)_{friction}]$ – from the Churchill equation for single-phase pressure drop (Churchill, 1977), with two-phase friction factor from Smith (1986),
- *heat transfer coefficient in condensation* $[\alpha_c]$ – from the Nusselt theory of condensation on a vertical surface (Mills, 1992), assuming a variable wall temperature distribution,
- *heat transfer for convection in the tube* $[\alpha_L]$ – from the Engineering Sciences Data Unit correlation for single-phase convection (Engineering Sciences Data Unit, 1967; Engineering Sciences Data Unit, 1968), and the Chen correlation for boiling heat transfer (Chen, 1966),
- *subcooled boiling criterion* – the critical wall temperature for the initiation of bubble formation, T^* , is calculated as given in Smith (1986); the condition $T_{w2} > T^*$ activates the nucleate boiling term in the Chen correlation,
- *saturated nucleate boiling criterion* – when the boiling point of the juice, T_{bp} , is reached, the condition $T_L > T_{bp}$ activates the Reynolds number factor, F , in the Chen correlation,
- *juice physical properties* – assumed to be temperature and composition dependent.

Numerical solution of the model

Numerical solution of ordinary differential equations is fairly routine, provided all the boundary conditions are given at one end of the evaporator tube. This is known as an *initial value problem*. However, the system under consideration here has boundary conditions at both boundaries, ie at either end of the evaporator tube, and thus requires more advanced solution techniques. The starting point of integration is the bottom of the evaporator tube; however, the system pressure and flow rate of condensate are only known at the top of the tube. This is known as a *two-point boundary value problem*. There are several available numerical methods for solving boundary value problems of this type (Davis, 1984; Na, 1979). For this study, a shooting method based on the Newton-Raphson technique was used. In essence, the numerical solution procedure used to solve the boundary value problem is as follows:

- A guess is made of the values of the unknown quantities at the bottom of the tube (ie pressure and flow rate of condensate per unit width).
- The system of ordinary differential equations is numerically integrated up the length of the tube, as if the problem were an initial value problem. Appropriate correlations for pressure drop and heat transfer are used to determine the change in pressure and enthalpy of the juice/vapour mixture within the tube over each of the differential height elements (δz) until the top of the tube is reached.
- The resulting values of pressure and flow rate of condensate at the top of the tube are compared to the known values of these quantities.
- If the values are found to differ, a more refined guess, utilising the Newton-Raphson technique, is made of these quantities at the bottom of the tube and the sequence is repeated.

A fourth-order Runge-Kutta method with an automatically controlled step size was used to perform the numerical integration.

The evaporator model was used to develop an evaporator simulation program in the MATLAB programming language. The inputs required by this program for the simulation of a climbing film evaporator system are:

- physical parameters of the evaporator system to be modelled, such as the number of tubes, inner and outer tube diameters, tube length, tube surface roughness and the thermal conductivity of the tube material,
- operational parameters of the evaporator system, such as the flow rate of juice fed to the bottom of the evaporator, brix and purity of the feed juice, temperature of the feed juice entering the tubes, vapour pressure in the headspace of the evaporator and the steam pressure in the calandria.

The outputs provided by the program are profiles of the following quantities as they vary over the length of the tube:

- the two state variables involved in the integration of the ordinary differential equations, namely mixture enthalpy and pressure
- flow rate of condensate on the outer tube wall
- temperatures of the steam, outer tube wall, inner tube wall and juice/vapour mixture within the tube
- brix of the liquid phase within the tube
- heat transfer coefficients for condensation on the outside of the tube and for boiling within the tube
- mass flow rates of the vapour and liquid phases within the tube

- pressure within the tube
- two-phase mixture quality within the tube
- heat flux across the tube wall.

Experimental data and preliminary model verification

Experimental data from the Felixton pilot plant climbing film evaporator were used to test the proposed model. The experimental data utilised were those obtained from the first effect factorial experiment, in which pure sucrose solutions were evaporated over the range of operating conditions usually encountered in first effect evaporators in the South African sugar industry (Walthew and Whitelaw, 1996). Details of the experimental apparatus are described elsewhere (Walthew *et al.*, 1995). The variables selected for manipulation during the factorial experiment were steam pressure, vapour pressure, juice flow rate and juice feed temperature and brix. The steam and vapour pressures were manipulated to give a fixed temperature difference across the tube wall. The values of these variables used in the factorial experiment are given in Table 1.

Table 1
Operating conditions for factorial experiment

Operating variable	Low	High
Temperature difference [°C]	4,0	7,5
Feed juice flow rate [kg/s]	0,042	0,075
Feed juice temperature [°C]	102,0	110,0
Feed juice brix [%]	8,0	13,0

It was found that the simulation results did not agree with those obtained by experiment. In general, the simulation program under-predicted the heat transfer actually occurring in the pilot plant evaporator. In other words, the simulation program predicted lower heat transfer coefficients, condensate flow rates, exit brixes, vapour flow rates, heat fluxes and two-phase mixture qualities than had been observed in the experimental data.

Careful analysis of the heat transfer correlations used in the evaporator model showed that the cause of the low heat transfer coefficients was the Chen correlation for flow boiling in vertical tubes. This correlation consists of two terms; one to account for convective heat transfer to the boiling fluid, and the other for the heat transfer to the fluid during bubble formation. While the convective heat transfer term was considered to be accurate, it was felt that the modified Forster-Zuber equation, used by the Chen correlation to account for heat transfer during bubble formation (Forster and Zuber, 1955), was inaccurate. An attempt was thus made to replace this outdated, inaccurate term with a more modern equation of greater accuracy. A literature survey was performed on the topic of flow boiling in vertical tubes. It was found that none of the available correlations (Cooper, 1989; Dhir, 1991; Gorenflo, 1994; Gungor and Winterton, 1986; Kenning and Cooper, 1989; Klimenko, 1988; Shah, 1982; Steiner and Taborek, 1992; Webb and Gupte, 1992) could be applied to the conditions used in the South African sugar industry, due to the extremely low juice flow rates commonly used. Some of the more promising correlations were tested for incorporation into the model, but were found to be inadequate. It was thus found to be impossible to replace the Forster-Zuber equation with a correlation of greater accuracy.

Rigorous model identification

The Forster-Zuber equation, as used in the Chen correlation,

$$\alpha_{FZ} = k_{FZ} \cdot \frac{\Delta T_{sat}^{0,24} \Delta p_{sat}^{0,75} c_{pl}^{0,45} \rho_L^{0,49} \lambda_L^{0,79}}{\sigma^{0,5} h_{LG}^{0,24} \eta_L^{0,29} \rho_G^{0,24}} \quad (8)$$

contains a constant parameter, k_{FZ} , traditionally quoted with a surprisingly high accuracy. A value of 0,0015 originally reported by Forster and Zuber (1955) and later reduced by Chen (1966) to 0,00122, is commonly accepted as being applicable to a wide range of fluids and heating surfaces. In contrast, the value of a similar coefficient in the Rohsenow correlation (Rohsenow, 1952), as provided in the literature, was found to vary greatly (Mills, 1992), depending on the nature of the fluid being boiled and the surface at which the boiling takes place (Table 2). It can be inferred from this table that the nature of the fluid being boiled and the surface characteristics of the evaporator tube may greatly influence k_{FZ} . It was thus decided to utilise the Forster-Zuber constant (being the most uncertain parameter in the proposed model) as the parameter to be *optimised* in order to improve the accuracy of the model predictions. It was felt that this approach was justified, for the following reasons:

- there is a large degree of variability present in the data published in the literature on the topic of nucleate boiling (personal communication). Heat transfer coefficient predictions for nucleate boiling may vary from correlation to correlation by more than 1 900% (Hewitt *et al.*, 1994).
- most nucleate boiling correlations are inapplicable to the conditions normally encountered in the South African sugar industry, due to the low flow rates normally used (1,2,3,4 personal communications).

Table 2
Values of the constant parameter in the Rohsenow correlation

Boiling liquid	Surface	Value of parameter
Water	Copper, scored	0,0068
Water	Copper, polished	0,0130
Water	Brass	0,0060
Benzene	Chromium	0,0100
Isopropyl alcohol	Copper	0,0023

In essence, the least-squares optimisation algorithm used for the improvement of the model accuracy consisted of the identification of a new constant in the Forster-Zuber equation which would minimise a specially defined *performance index* (or *objective function*), and result in a better fit of the experimental data from the pilot plant evaporator under study. The performance index represented a weighted deviation of the model predictions from the corresponding experimental output values. In addition, since it was found that several experimental input parameters to the model were subject to experimental error, rather than being unconditionally reliable, the performance index was expanded by including additional data reconciliation terms. Thus, its final form was:

¹ RHS Winterton, School of Manufacturing and Mechanical Engineering, Birmingham University, Birmingham B15 2TT, United Kingdom

² H Müller-Steinhagen, Chemical and Processing Engineering, University of Surrey, Guildford, Surrey GU2 5XH, United Kingdom

³ D Steiner, Universität Karlsruhe, Postfach 6980, Kaiserstraße 12, D-76128, Karlsruhe, Germany

⁴ K Stephan, Institut für Technische Thermodynamik und Thermische Verfahrenstechnik, Universität Stuttgart, 70550 Stuttgart, Germany

$$\begin{aligned}
 INDEX = & \frac{(VP - \overline{VP})^2}{var(\overline{VP})} + \frac{(SB - \overline{SB})^2}{var(\overline{SB})} + \frac{(VF - \overline{VF})^2}{var(\overline{VF})} \\
 & + \frac{(SF - \overline{SF})^2}{var(\overline{SF})} + \frac{(ICF - \overline{ICF})^2}{var(\overline{ICF})} + \frac{(FR - \overline{FR})^2}{var(\overline{FR})} \\
 & + \frac{(FT - \overline{FT})^2}{var(\overline{FT})} + \frac{(BP - \overline{BP})^2}{var(\overline{BP})} + \frac{(FB - \overline{FB})^2}{var(\overline{FB})} \\
 & + \frac{(CF - \overline{CF})^2}{var(\overline{CF})} \quad (9)
 \end{aligned}$$

where the overscore indicates an experimentally measured value. The variances $var(x)$ were determined by statistically analysing the fluctuations of the respective variables during continuous steady state operation of the pilot plant. Consequently, the performance index was not only optimised with respect to the Forster-Zuber constant, k_{FZ} , but also with respect to the following set of operating input conditions characterising the experimental run under investigation:

- feed juice flow rate
- feed juice temperature
- feed juice brix
- pressure at the bottom of the evaporator tubes
- steam condensate flow rate.

Table 3
Operating conditions used in simulation

Run number	Feed juice flow rate [kg/s]	Feed juice brix [%]	Feed juice temperature [°C]	Vapour pressure [kPa]	Steam pressure [kPa]
1	0,0175	8,0	96,31	151,30	173,49
2	0,0183	13,0	105,73	151,28	196,34
3	0,0252	12,9	102,52	151,31	196,32
4	0,0142	8,0	100,73	151,36	173,45
5	0,0147	12,9	108,42	151,38	195,50
6	0,0233	13,0	108,65	151,33	196,27
7	0,0237	13,0	107,02	151,36	194,88
8	0,0236	8,0	109,29	151,32	173,34
9	0,0252	8,0	106,92	151,35	191,76
10	0,0148	8,0	102,01	151,32	183,83

The index was optimised separately for each of the ten experimental runs studied (Table 3), using the Marquardt-Levenberg optimisation routine (Marquardt, 1963; Levenberg, 1944). These optimisations resulted, firstly, in optim-

ised values of k_{FZ} and, secondly, in refined values for the aforementioned set of experimental input conditions. The results of the extensive computations have been summarised in Table 4.

Results and discussion

It was found that the calculated optimal values of the Forster-Zuber constant were several times higher than Chen's value of 0,00122, ranging from 0,003 to 0,009. Typically, lower values of k_{FZ} (0,003 to 0,005) occurred for experimental runs characterised by a high change in brix over the evaporator (15 to 30%), whereas runs yielding a slight increase in brix (3 to 5%) resulted in higher values of k_{FZ} (0,007 to 0,009). This behaviour was found to be strongly correlated with the average heat flux across the evaporator tube (Figure 2). However, the hypothesis of a relationship between heat flux and the value of k_{FZ} seems to be premature and more experimental work is needed to investigate it fully.

In the light of the extremely large uncertainties associated with the published values of k_{FZ} , the values obtained in this study were found to be fairly consistent. Moreover, since the data fit for individual tests was found to be particularly good, it would seem that, while a global model identification involving all of the experimental runs together would result in slightly poorer (on average) predictions at a compromised value of k_{FZ} , the fit would still be acceptable. In fact, an extensive computational study of this nature is already in progress.

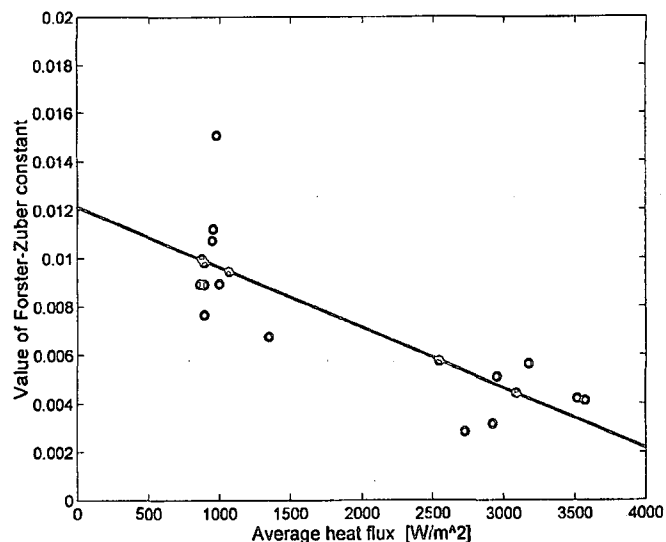


FIGURE 2: Variation of the calculated Forster-Zuber constant with heat flux.

Table 4
Final simulation results

Run no.	Total mass flow rate [kg/s]		Feed juice temperature [°C]		Vapour pressure [kPa]		Bottom pressure [kPa]		Feed juice brix [%]	
	Exptl.	Calc.	Exptl.	Calc.	Exptl.	Calc.	Exptl.	Calc.	Exptl.	Calc.
1	0,0175	0,0175	96,31	96,28	151,30	153,51	202,00	197,93	8,0	8,1
2	0,0183	0,0171	105,73	105,95	151,28	156,69	167,40	167,41	13,0	14,1
3	0,0252	0,0248	102,52	105,24	151,31	155,62	167,68	168,94	12,9	13,7
4	0,0142	0,0142	100,73	100,67	151,36	155,55	201,88	197,86	8,0	8,2
5	0,0147	0,0138	108,42	113,15	151,38	154,06	159,52	162,38	12,9	14,1
6	0,0233	0,0227	108,65	112,81	151,33	151,28	158,82	160,37	13,0	14,3
7	0,0237	0,0230	107,02	108,74	151,36	149,43	157,70	159,45	13,0	14,3
8	0,0236	0,0238	109,29	107,71	151,32	151,24	183,58	180,88	8,0	8,2
9	0,0252	0,0250	106,92	107,22	151,35	155,10	167,42	167,67	8,0	8,7
10	0,0148	0,0144	102,01	99,81	151,32	152,71	166,78	165,78	8,0	9,7

Table 4 (continued)

Run no.	Product syrup brix [%]		Steam condensate flow rate [kg/s]		Vapour product flow rate [kg/s]		Product syrup flow rate [kg/s]		Condensate flow at tube top [kg/s]		Forster-Zuber const. (x1000)
	Exptl.	Calc.	Exptl.	Calc.	Exptl.	Calc.	Exptl.	Calc.	Exptl.	Calc.	
1	9,5	9,5	0,0031	0,0030	0,0028	0,0025	0,0147	0,0150	0	4x10 ⁻⁷	8,94
2	32,1	31,6	0,0092	0,0097	0,0109	0,0094	0,0074	0,0077	0	-5x10 ⁻⁶	5,63
3	22,1	21,6	0,0092	0,0095	0,0105	0,0090	0,0147	0,0157	0	-7x10 ⁻⁶	4,43
4	9,9	9,7	0,0028	0,0026	0,0027	0,0023	0,0115	0,0119	0	4x10 ⁻⁷	8,92
5	40,0	39,7	0,0084	0,0090	0,0099	0,0089	0,0048	0,0049	0	-7x10 ⁻⁶	3,15
6	27,7	27,0	0,0104	0,0108	0,0124	0,0107	0,0109	0,0120	0	-5x10 ⁻⁶	4,20
7	27,3	26,7	0,0105	0,0109	0,0124	0,0107	0,0113	0,0123	0	-7x10 ⁻⁶	4,12
8	10,1	9,9	0,0043	0,0041	0,0048	0,0039	0,0188	0,0199	0	2x10 ⁻⁶	6,75
9	13,7	13,3	0,0090	0,0090	0,0105	0,0087	0,0147	0,0163	0	-2x10 ⁻⁶	5,10
10	20,9	19,9	0,0079	0,0078	0,0092	0,0074	0,0057	0,0070	0	4x10 ⁻⁷	5,75

A comparison of the model predictions with the experimental data for ten different runs was given in Table 4. In order to illustrate some of these results graphically, data from run 2 are shown in Figure 3. All of the key output variables, ie product syrup brix and flow rate, vapour product flow rate, steam condensate flow rate and product vapour pressure could be predicted to within a ±5% relative error. Additionally, the distribution of the local overall heat transfer coefficient (HTC) along the tube length (solid line in the last graph

of Figure 3) was found to be in good agreement with the average experimental HTC value (dashed line) calculated for the pilot plant (Walthev *et al.*, 1996).

Figure 4 shows the predicted distribution of temperatures (steam, outer and inner wall, and juice) along the tube length for run 2. The juice temperature profile exhibits a discontinuity of slope at a height of approximately 0,3 m up the tube, which represents the transition from the subcooled to the saturated nucleate boiling regime.

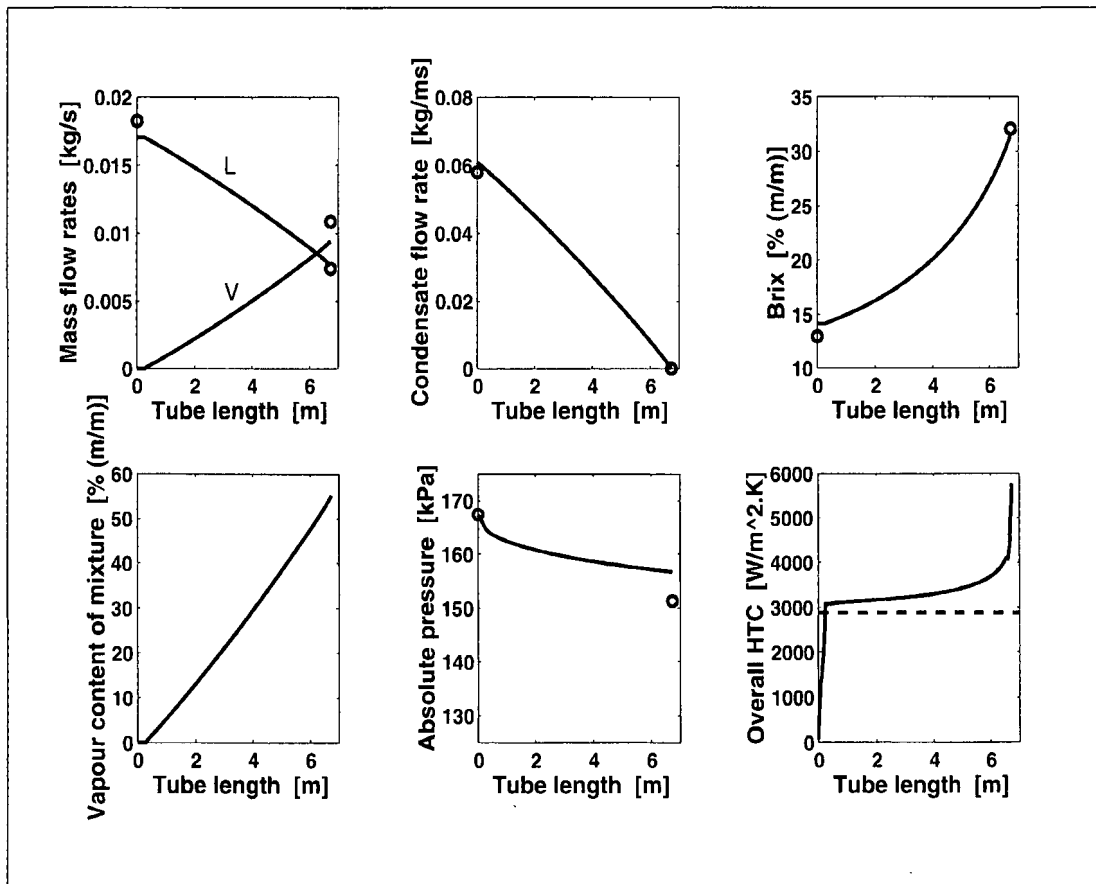


FIGURE 3: Simulation results for experimental run 2.

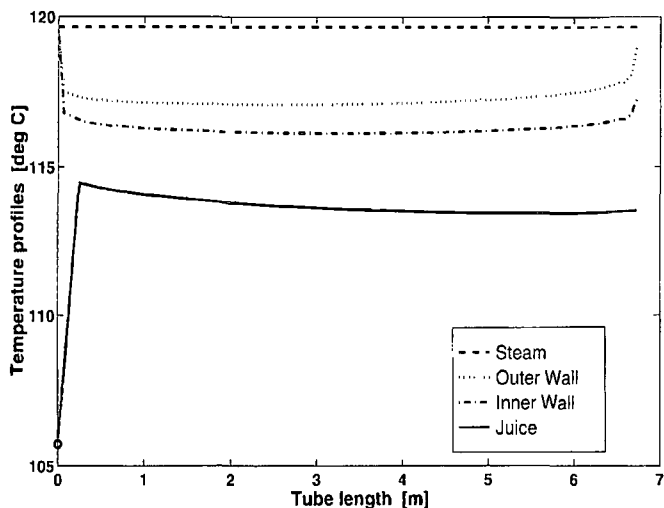


FIGURE 4: Simulated temperature profile results for experimental run 2.

Figure 5 shows the difference in the distribution of heat transfer parameters (such as temperature profiles, syrup brix and overall HTC) as they vary along the tube, depending on the operating conditions of the evaporator. Plots (a), (b) and (c) of Figure 5 show the results from run 4, characterised by a

low steam temperature. It can be seen that almost half of the tube still functions as a juice preheater, with resulting low local overall HTC values being observed (mostly due to the laminar flow nature of the convection on the juice side, as a result of the low juice flow rate). The rest of the tube performs the evaporation. Obviously, these conditions resulted in a very poor final brix value. In contrast, run 10 (displayed in graphs (d), (e) and (f) of Figure 5) was carried out under a higher steam temperature. This resulted in a high overall HTC being observed over almost the entire length of the tube, yielding a high syrup product brix. Both HTC profiles shown in Figure 5 display two characteristic discontinuities in slope. The first occurs at the transition from single-phase convection to subcooled boiling. The second occurs at the onset of saturated nucleate boiling. The dramatic HTC increase which can be observed at the end of the profile can be explained by the absence of condensate on the outer tube wall at the top of the evaporator.

Conclusions

A series of experimental runs was carried out on a pilot plant climbing film evaporator at the Felixton mill to investigate the efficiency of heat transfer under varying operating conditions (Walthev and Whitelaw, 1996). The factorial experiment involving changes of feed juice flow rate, brix and

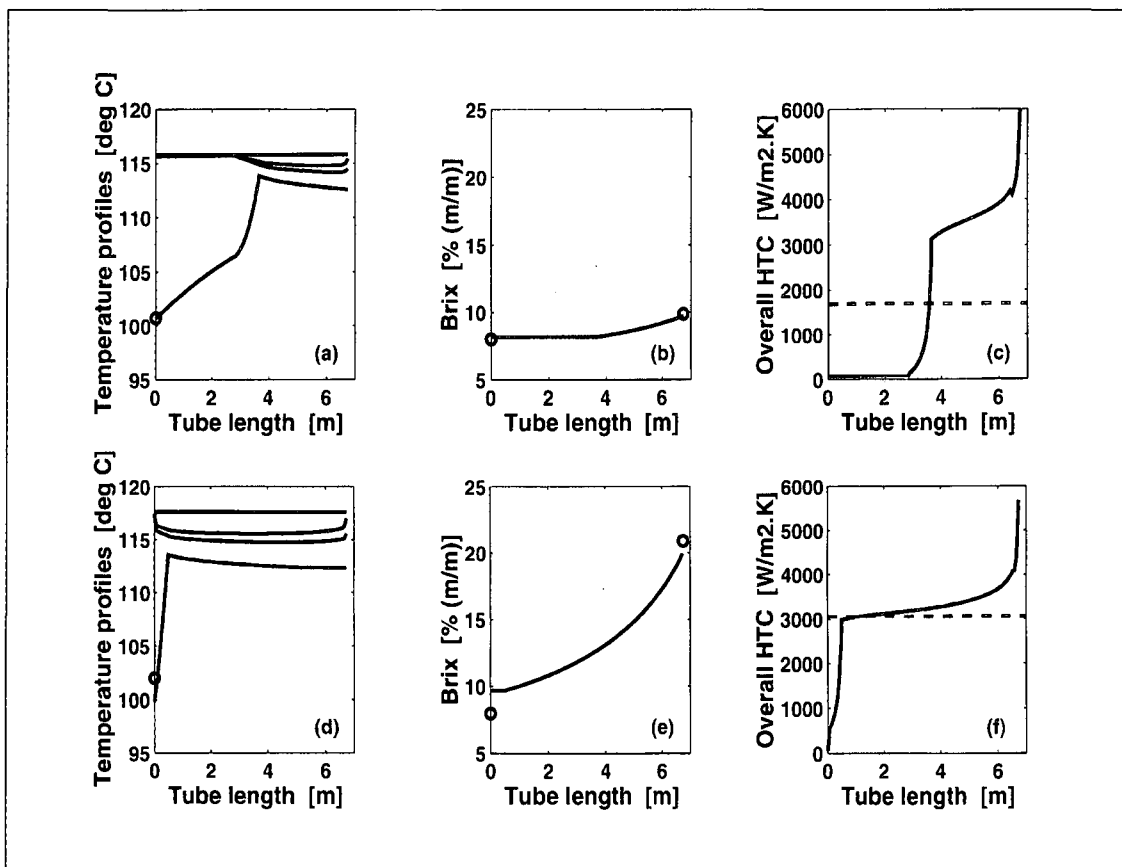


FIGURE 5: Comparison of simulation results for experimental runs 4 and 10.

temperature, head space vapour pressure and raw steam pressure resulted in a set of output data which was used to identify a mathematical model of the evaporator. The initially adopted model utilised the Chen correlation for boiling heat transfer in vertical tubes. However, the results of computer simulation were found to represent the experimental data inadequately. It was thus decided to modify the Chen correlation by adapting the Forster-Zuber constant, k_{FZ} , in the nucleate boiling term. The identification of this constant led to a great improvement in the model performance, giving $\pm 5\%$ relative error between model predictions and experimental measurements. A variation in the value of k_{FZ} was also observed and could be correlated with heat flux.

Currently, the developed model can be used to simulate climbing film evaporator performance under various conditions. Apart from changes in traditional operating variables such as steam pressure, feed juice flow rate, and feed juice temperature etc. the model can also predict the system performance for such inconvenient changes in practice as those of tube size and material. The presence of fouling may also be accounted for if the thermal properties of the scale are known.

REFERENCES

- Bourgeois, J and Le Maguer, M (1983). Modelling of heat transfer in a climbing-film evaporator: part I. *J Food Eng* 2: 63-75.
- Chen, JC (1966). Correlation for boiling heat transfer to saturated fluids in convective flow. *I&EC Proc Des Dev* 5: 322-329.
- Churchill, SW (1977). *Chem Eng.* 7 November, 84: 91-92.
- Cooper, MG (1989). Flow boiling – the ‘apparently nucleate’ regime. *Int J Heat Mass Transfer* 32: 459-464.
- Davis, ME (1984). *Numerical Methods and Modelling for Chemical Engineers*. Wiley House Publishers, New York, 258 pp.
- Dhir, VK (1991). Nucleate and transition boiling heat transfer under pool and external flow conditions. *Int J Heat Fluid Flow* 12: 290-314.
- Engineering Sciences Data Unit (1967). Forced convection heat transfer in circular tubes, Part 1: Correlations for fully developed turbulent flow – their scope and limitations. ESDU Item 68006.
- Engineering Sciences Data Unit (1968). Forced convection heat transfer in circular tubes, Part 2: Data for laminar and transitional flows, including free-convection effects. ESDU Item 68007.
- Forster, HK and Zuber, N (1955). Dynamics of vapor bubbles and boiling heat transfer. *AIChE J* 1: 531-535.
- Gorenflo, D (1994). Behältersieden, *VDI Wärmeatlas*, Section Ha, 7th ed, VDI-Verlag.
- Gungor, KE and Winterton, RHS (1986). A general correlation for flow boiling in tubes and annuli. *Int J Heat Mass Transfer* 29: 351-358.
- Gupta, AS and Holland, FA (1966). Heat transfer studies in a climbing film evaporator. Part I. Heat transfer from condensing steam to boiling water. *Canad J Chem Eng* 44: 77-81.
- Hewitt, GF, Shires, GL and Bott, TR (1994). *Process Heat Transfer*. CRC Press, Boca Raton, 445-448.
- Kenning, DBR and Cooper, MG (1989). Saturated flow boiling of water in vertical tubes. *Int J Heat Mass Transfer* 32: 445-458.
- Klimenko, VV (1988). A generalized correlation for two-phase forced flow heat transfer. *Int J Heat Mass Transfer* 31: 541-552.
- Levenberg, K (1944). *Q Appl Math* 2: 164-168.
- Marquardt, DW (1963). *J SIAM* 11: 431-441.
- Mills, AF (1992). *Heat Transfer*. International student edition, Irwin Publishers, Boston, 596-604.
- Na, TY (1979). *Computational methods in engineering boundary value problems*. Academic Press, New York, 309 pp.
- Rohsenow, WM (1952). A method of correlating heat transfer data for surface boiling of liquids. *Trans ASME* 74: 969.
- Shah, MM (1982). Chart correlation for saturated boiling heat transfer. *ASHRAE Trans* 88: 185-196.
- Smith, RA (1986). *Vaporisers: selection, design and operation*. Longman, New York: 189-191.
- Steiner, D and Taborek, J (1992). Flow boiling heat transfer in vertical tubes correlated by an asymptotic method. *Heat Trans Eng* 13: 43-69.
- Walthew, DC and Whitelaw, RW (1996). Factors affecting the performance of long tube climbing film evaporators. *Proc S Afr Sug Technol Ass* 70 (in press).
- Walthew, DC, Lionnet, GRE and Whitelaw, RW (1996). Progress report on the FX pilot plant: A factorial investigation into first effect operation. Sugar Milling Research Institute Technical Report (in press).
- Walthew, DC, Whitelaw, RW and Peacock, SD (1995). Preliminary results from a long tube climbing film pilot evaporator. *Proc S Afr Sug Technol Ass* 69: 132-137.
- Webb, RL and Gupte, NS (1992). A critical review of correlations for convective vaporization in tubes and tube banks. *Heat Trans Eng* 13: 58-81.
- Zinemanas, D, Hasson, D and Kehat, E (1984). Simulation of heat exchangers with change of phase. *Comput Chem Eng* 8: 367-375.

Nomenclature

- A = cross sectional area for flow within the tube [m^2]
- α_c = local heat transfer coefficient in condensation on the outer tube wall [$W/m^2 \cdot K$]
- α_L = local heat transfer coefficient within the tube [$W/m^2 \cdot K$]
- BP = pressure at the bottom of the tubes of the pilot plant evaporator [Pa]
- C_{pl} = heat capacity of the liquid phase within the tube [$J/kg \cdot K$]
- CF = mass flow rate of condensate from the pilot plant evaporator [kg/s]
- D_{in} = inner diameter of the evaporator tube [m]
- D_{out} = outer diameter of tube [m]
- F_0 = total mass flowrate (liquid and vapour) within the tube [kg/s]
- FB = brix of feed juice to the pilot plant evaporator [% (m/m)]
- FR = mass flow rate of feed juice to the pilot plant evaporator [kg/s]
- FT = temperature of feed juice to the pilot plant evaporator [$^{\circ}C$]
- h_{Lg} = latent heat of vapourisation of juice [J/kg]
- H = specific enthalpy of the juice/vapour mixture [J/kg]
- H_c = specific enthalpy of condensate film on the outside of the tube [J/kg]
- ICF = initial mass flow rate of condensate at the top of the tubes of the pilot plant evaporator [kg/s]
- k_{FZ} = parameter in Forster-Zuber equation
- L = mass flowrate of liquid within the tube [kg/s]
- λ_L = thermal conductivity of the liquid phase within the tube [$W/m \cdot K$]
- η_L = viscosity of the liquid phase within the tube [$Pa \cdot s$]
- p = pressure within the tube [Pa]
- Δp_{sat} = difference in vapour pressure corresponding to ΔT_{sat} [Pa]
- ρ_g = density of the vapour phase within the tube [kg/m^3]
- ρ_L = density of the liquid phase within the tube [kg/m^3]
- ρ_m = density of the juice/vapour mixture within the tube [kg/m^3]
- $q_{condens}$ = heat flux through the tube wall due to condensation of steam [W/m^2]
- $q_{conduct}$ = heat flux through the tube wall due to conduction [W/m^2]
- q_{conv} = heat flux through the tube wall due to convection within the tube [W/m^2]
- r = mass fraction non-sucrose dissolved solids in the liquid phase within the tube [-]
- s = mass fraction sucrose in the liquid phase within the tube [-]
- SB = brix of syrup from the pilot plant evaporator [% (m/m)]

SF	= mass flow rate of syrup from the pilot plant evaporator [kg/s]	V	= mass flowrate of vapour within the tube [kg/s]
σ	= surface tension of juice/vapour [N/m]	$var(x)$	= the variance (or weighting) of experimental input variable x , as used in the optimisation algorithm
T_L	= temperature of the juice/vapour mixture within the tube [°C]	VF	= mass flow rate of product vapour from the pilot plant evaporator [kg/s]
T_s	= temperature of the condensing steam [°C]	VP	= headspace vapour pressure of the pilot plant evaporator [Pa]
T_{w1}	= temperature of the outer tube wall [°C]	z	= vertical position in the evaporator tube [m]
T_{w2}	= temperature of the inner tube wall [°C]		
ΔT_{sat}	= wall superheat [°C]		